BRAZILIAN JOURNAL
OF MEDICAL AND BIOLOGICAL RESEARCH
www.bjournal.com.br

ISSN 0100-879X
Volume 44 (2) 84-181 February 2011
BIOMEDICAL SCIENCES

doi: 10.1590/S0100-879X2010007500132

Braz J Med Biol Res, February 2011, Volume 44(2) 91-99

The effect of down-regulation of Smad3 by RNAi on hepatic stellate cells and a carbon tetrachloride-induced rat model of hepatic fibrosis

Z.R. Wang, J.H. Wang, C.L. Hu, W.G. Cao, X.J. Shen, M.Y. Wu, L. Shen and S.L. Wu

Brazilian Journal of Medical and Biological Research (2011) 44: 91-99
ISSN 0100-879X

The effect of down-regulation of Smad3 by RNAi on hepatic stellate cells and a carbon tetrachloride-induced rat model of hepatic fibrosis

Z.R. Wang[1,2], J.H. Wang[1], C.L. Hu[1], W.G. Cao[2], X.J. Shen[2], M.Y. Wu[2], L. Shen[1] and S.L. Wu[1]

[1]Department of Biochemistry and Molecular Biology, Soochow University, Suzhou, China
[2]The Fifth People's Hospital of Suzhou, Suzhou, China

Abstract

Searching for effective Smad3 gene-based gene therapies for hepatic fibrosis, we constructed siRNA expression plasmids targeting the rat Smad3 gene and then delivered these plasmids into hepatic stellate cells (HSCs). The effect of siRNAs on the mRNA levels of Smad2, Smad3, Smad4, and collagens I-α1, III-α1 and IV-α1 (Col1α1, Col3α1, Col4α1, respectively) was determined by RT-PCR. Eighty adult male Sprague-Dawley rats were randomly divided into three groups. Twice a week for 8 weeks, the untreated hepatic fibrosis model (N = 30) and the treated group (N = 20) were injected subcutaneously with 40% (v/v) carbon tetrachloride (CCl_4)-olive oil (3 mL/kg), and the normal control group (N = 30) was injected with olive oil (3 mL/kg). In the 4th week, the treated rats were injected subcutaneously with liposome-encapsulated plasmids (150 µg/kg) into the right liver lobe under general anesthesia once every 2 weeks, and the untreated rats were injected with the same volume of buffer. At the end of the 6th and 8th weeks, liver tissue and sera were collected. Pathological changes were assessed by a semi-quantitative scoring system (SSS), and a radioimmunoassay was used to establish a serum liver fibrosis index (type III procollagen, type IV collagen, laminin, and hyaluronic acid). The mRNA expression levels of the above cited genes were reduced in the HSCs transfected with the siRNA expression plasmids. Moreover, in the treated group, fibrosis evaluated by the SSS was significantly reduced ($P < 0.05$) and the serum indices were greatly improved ($P < 0.01$). These results suggest that Smad3 siRNA expression plasmids have an anti-fibrotic effect.

Key words: Smad3; SiRNA; Hepatic fibrosis; Carbon tetrachloride

Introduction

Hepatic fibrosis is a common pathological process involved in chronic hepatopathy, including cirrhosis. Its main feature is an imbalance in the synthesis and degradation of extracellular matrix (ECM), which leads to a great deal of precipitation in the perisinusoidal space (space of Disse). It is currently thought that the activation of hepatic stellate cells (HSCs) is not only the key link in the development of hepatic fibrosis, but also the main source of ECM (1-6). Transforming growth factor beta 1 (TGF-β1) is the most powerful enhancing factor in hepatic fibrosis (7-9). TGF-β1 combines with receptors and forms TβRII-TGF-β1-TβRI hetero-oligomeric complexes. It then activates downstream Smad signaling molecules and modulates the transcription of target genes (e.g., the collagen gene). In this process, the activation of Smad3 has a great impact on both the subsequent HSC phenotype and the synthesis of collagen. Thus, the TGF-β1-Smad3 signaling pathway plays an important role in ECM synthesis in activated HSCs (10-12). Although the role of TGF-β1-Smad3 is clear, methods by which to harness this pathway in hepatic fibrosis treatment have not been characterized.

It is now recognized that cells contain a variety of RNA species. Small nuclear RNAs are believed to regulate protein production by a variety of mechanisms, including the regulation of protein translation and mRNA stability. By preparing appropriately sized RNAs of the correct specificity, it is possible to utilize this pathway to induce the degradation of mRNAs in

Correspondence: S.L. Wu, Department of Biochemistry and Molecular Biology, Soochow University, 215123 Suzhou, China.
Fax: +86-512-6588-0407. E-mail: shiliang_wu@126.com

Received June 25, 2010. Accepted November 12, 2010. Available online November 26, 2010. Published February 7, 2011.

a highly specific manner. The siRNA method was adopted to down-regulate Smad3 gene expression, and Smad3 siRNA expression vectors were constructed. The plasmids were transfected into a rat hepatic fibrosis model induced by carbon tetrachloride (CCl_4) with positive liposomes to inhibit TGF-β1-Smad signaling. The impact of this approach on HSC fibrosis and the hepatic fibrosis model was evaluated.

Material and Methods

Material

HSC-T6 rats were purchased from the Institute of Biochemistry and Cell Biology, Shanghai Institutes for Biological Sciences, Chinese Academy of Sciences. Eighty adult male Sprague-Dawley rats (60 to 65 days of age, weighing 160-180 g, Lot No.: SCXK (Su) 2007-0007) were provided by the Animal Center Laboratory of Soochow University. The use of animals in this study was approved by the Animal Ethics Committee of Soochow University and the protocol of animal treatment was approved by the Institutional Animal Care and Use Committee.

Calf serum was purchased from Huamei (China); complete Dulbecco's modified Eagle's medium (DMEM) was purchased from Gibco (USA); trypsin was purchased from Sigma (USA); Diethylpyrocarbonate was purchased from Huashun (China); oligo (dT), RNase inhibitor, superscript II RNase H reverse transcriptase, Taq Dnase, dNTP mixture (10 mM), 10X PCR buffer and $MgCl_2$ (25 mM) were purchased from Promega (China); agarose and mix DNA marker were purchased from Ferment (China); M-MLV reverse transcriptase, *Hin*dIII, *Bam*HI and T4-ligase were purchased from MBI Fermentas (Lithuania); trizol and lipofectamine 2000 were purchased from Invitrogen (USA); rat Smad3 monoclonal antibody was purchased from Santa Cruz (USA); goat anti-mouse IgG-HRP (horseradish peroxidase) was purchased from Biyuntian (China); hyaluronic acid (HA), laminin (LN), type III procollagen (PCIII), type IV collagen (IVC), and a radioimmunoassay kit were purchased from Haiyan (China); antigen-removing solution of sodium citrate CCl_4, citrate sodium buffer solution, diaminobenzidine, streptavidin-biotin complex and antibodies against collagen types I, III, and IV were purchased from Boshide (China).

The primers were designed by Genetyx and synthesized after homology searching by GeneBank BLAST (Table 1). The Smad3 primers were synthesized by Jinsite (China). The actin, GAPDH, TGF-β, Smad2, 3, 4, and collagen I-α1, III-α1, IV-α1 (Col1α1, Col3α1, Col4α1, respectively) primers were synthesized by Invitrogen (China).

Construction of smad3 siRNA expression vectors

Three siRNA sequences targeting rat Smad3 (GeneBank accession No. NM_013095) were designed using the Ambion software produced by GenePharma Co., Ltd., China (Table 2). Positive-sense and anti-sense DNA oligonucleotides were synthesized according to the protocol provided by the SilenCircle RNAi Kit (Qiagen, Ltd., UK) (Table 3). The DNA fragments corresponding to the target gene were amplified by PCR. The up (+) underlined position is a *Hin*dIII restriction site and the down (-) underlined position is a *Bam*HI restriction site. The PCR product and the eukaryotic expression vector pRNAT-U6.1/Neo were mixed together and digested with *Hin*dIII and *Bam*HI. A T4 ligase reaction system was used to connect the appropriately digested oligonucleotide and expression vector in recombinant clone ligation buffer. Competent DH5α cells were transformed with the ligated products and allowed to grow in culture. The cells were screened for positive clones. DNA was harvested from the positive clones and subjected to sequencing analysis (Shanghai Invitrogen, Co., China).

Cell culture

Rat HSC-T6 cells were maintained at 37°C in DMEM supplemented with 10% fetal calf serum, 100 U/mL penicillin, and 100 U/mL streptomycin, under a 5% CO_2 atmosphere.

Transfection optimization

Rat HSC-T6 cells in the logarithmic growth phase were seeded into a 25-mL dish. Once cell confluence reached 70%, different amounts of the plasmids (i.e., 0.4, 0.6, 0.8, 1.0, 1.2 μg plasmids/10^6 cells) were transfected into HSCs using lipofectamine 2000. The medium was replaced with fresh culture medium at 12 h after transfection. HSCs were observed by fluorescence microscopy at 48 h post-transfection to identify

Table 1. PCR primer sequences of Smads, collagens (Col), GAPDH, and Actin.

Gene	Sense	Antisense	Length (bp)
Smad2	TATACCCACTCCATTCCA	ACTATCACTTAGGCACTCG	474
Smad3	ACAAGGTCCTCACCCAGATG	TGGCGATACACCACCTGTTA	347
Smad4	GGCTGGTCGGAAAGGATT	GTGGGTAAGGATGGCTGT	270
Col1α1	TTCCTGCCTCAGCCACCTCA	GAACCTTCGCTTCCATACTCG	431
Col3α1	ATGGTGGCTTTCAGTTCAG	CAATGTCATAGGGTGCGATA	351
Col4α1	GCTCAGCGTCTGGCTTCT	CCTCGTGTCCCTTTCGTT	270
GAPDH	AGAAGGCTGGGGCTCATTTG	AGGGGCCATCCACAGTCTTC	258
Actin	AGGCCCCTCTGAACCCTAAG	TGCCACAGGATTCCATACCC	501

Table 2. Three target sites for smad3 siRNA.

No.	Site (bp)	Target sequence
1	1316	aa ATCCGCATGAGCTTCGTCAAA
2	1289	aa TCTACCAGTTGACTCGCATGT
3	1330	aa GTCAAAGGCTGGGGAGCCGAG

the optimal transfection conditions.

RT-PCR

At 48 h post-transfection, total RNA was extracted from the HSCs with trizol according to manufacturer instructions. A total of 2 µg RNA was reverse transcribed in a 20-µL reaction solution containing 10 U M-MLV reverse transcriptase and 0.5 µg oligo (dT) primer. PCR of the cDNA was performed in 50 µL containing 4 µL 4X dNTPs, 2 U Taq DNA polymerase (MBI), and 20 nmol of each primer. The samples were amplified in 30 cycles of 9°C for 1 min, 5°C for 30 s, and 72°C for 1 min, followed by a single incubation at 72°C for 10 min. The GAPDH or actin gene was used as an internal control for standardization in triplicate.

Western blot analysis

At 48 h post-transfection, the cells were lysed with precooled lysis buffer and the protein content of the lysate was measured. Briefly, 20 µg protein was subjected to SDS-PAGE on a 10% polyacrylamide gel with a 5% stack solution at 80 mA for 2 h. The proteins were transferred to a membrane via a semidry transfer method for 2 h in standard transfer buffer. The membrane was blocked with 5% skim milk blocking buffer and then probed with protein-specific antibodies overnight at 4°C. The membrane was washed three times with Tris-buffered saline Tween-20, followed by incubation for 2 h with the appropriate HRP-conjugated secondary antibody at room temperature. An enhanced chemiluminescence kit was used for detection.

Preparation of the animal model and *in vivo* plasmid transfection

Eighty male Sprague-Dawley rats were randomized into three groups: normal control group (N = 30), untreated hepatic fibrosis group (N = 30), and treated hepatic fibrosis group (N = 20). Rats in the untreated and treated groups were injected subcutaneously in their back with a 40% (v/v) CCl_4-olive oil solution according to the following schedule: initial dose of 5 mL/kg followed by 3 mL/kg twice a week for 8 weeks. Rats in the normal group were injected with olive oil solution according to the same schedule. At the end of the 4th and 6th weeks, Smad3 siRNA plasmids (150 µg/kg) encapsulated in positive liposomes were injected subcutaneously into the right lobe of the liver of rats belonging to the treated group while under general anesthesia. Rats belonging to the untreated group were injected subcutaneously with the same volume of buffer (13,14).

Specimen preparation

In the untreated and normal groups, 10 rats were killed at the end of the 4th, 6th, and 8th weeks. In the treated group, 10 rats were killed and their sera were harvested at the end of the 6th and 8th weeks. Left lobe hepatic tissue was fixed in 10% formaldehyde solution, embedded in paraffin, sliced continuously at 4 µm, stained with hematoxylin and eosin and van Gieson stain, and observed under a light microscope. Hepatic fibrosis was graded according to a semi-quantitative scoring system (15-17) (Table 4).

Table 3. DNA oligos of positive-sense strand and anti-sense strand for the siRNA expression vectors.

siRNA	DNA fragment
1 A strand	5-gatcccTTTGACGAAGCTCATGCGGATttgatatccgATCCGCATGAGCTTCGTCAAAttttttccaaa-3
1 B strand	3-gAAACTGCTTCGAGTACGCCTAaactacaggcTAGGCGTACTCGAAGCAGTTTaaaaaaggttttcga-5
2 A strand	5-gatcccACATGCGAGTCAACTGGTAGAttgatatccgTGTACGCTCAGTTGACCATCTttttttccaaa-3
2 B strand	3-gTGTACGCTCAGTTGACCATCTaactacaggcAGATGGTCAACTGAGCGTACAaaaaaaggttttcga-5
3 A strand	5-gatcccCTCGGCTCCCCAGCCTTTGACttgatatccgGTCAAAGGCTGGGGAGCCGAGttttttccaaa-3
3 B strand	3-gGAGCCGAGGGGTCGGAAACTGaactacaggcCAGTTTCCGACCCCTCGGCTCaaaaaaggttttcga-5

Table 4. Semi-quantitative scoring system (SSS) for fibrosis.

Grade	Leaflet perisinusitis (L)	Portal area (P)	Fibrous septum	
			Number (N)	Width (W)
0	None	None	None	None
1	Limited and few	Expanded and aseptate	≤6/10 mm	Thin
2	Diffuse and numerous	Expanded and septate	>6/10 mm	Loose and wide
3	-	Cirrhosis	Cirrhosis	Compact and wide
4	-	-	-	≥2/3 biopsy area

Grading = L + P + 2 (N + W). There was only one fine fiber septum in the specimen. If there was only one fine fiber sptum in the specimen, W = 0.5; grading of the interval width was calculated as the average of the two measured widths.

Statistical analysis

Data are reported as means ± SD. Statistical comparisons were made by comparing means with an independent sample *t*-test. A P value of less than 0.05 indicated statistical significance. All statistical analyses were carried out using the SPSS 13.0 software.

Results

Construction of Smad3 siRNA expression vectors

A Smad3 PCR fragment and the pRNAT-U6.1/Neo vector were double-digested and the resulting products were purified and submitted to directional ligation. The ligation products were transformed and positive clones were identified by PCR using upstream and downstream primers that were designed on the basis of the vector of the targeted gene. Observation of a 347-bp PCR product indicated that the Smad3 siRNA oligonucleotide had been successfully inserted into the pRNAT-U6.1/Neo expression vector (Figure 1). Sequencing of positive clones showed that the Smad3 siRNA sequence and the corresponding Smad3 mRNA sequence published in Genebank (NM_013095) were identical, indicating successful construction of rat Smad3 siRNA eukaryotic expression vectors (i.e., SD1211-SiSmad3-1, SD1211-SiSmad3-2, SD1211-SiSmad3-3) (data not shown).

Identification of the optimal transfection concentration

The cells were transfected with five different concentrations of the siRNA eukaryotic expression plasmids. Fluorescence microscopy revealed that the fluorescence was strongest at 48 h post-transfection, and that the cell status was optimal after transfection with 1 µg plasmids/10^6 cells (Figure 2).

Identification of effective Smad3 siRNA expression vectors

Three different siRNA expression vectors (SD1211-SiSmad3-1, SD1211-SiSmad3-2, SD1211-SiSmad3-3) were transfected into HSCs. At 48 h post-transfection, the transfection efficiencies of the three vectors were above 85% as determined by fluorescence microscopy (Figure 3). The level of Smad3 mRNA expression in the HSCs was assessed after collecting the cells. Figure 4A demonstrates that the SD1211-SiSmad3-2 siRNA vector provided the most effective inhibition of Smad3 expression.

Silencing the efficacy of the SD1211-SiSmad3-2 siRNA vector

Smad3 protein expression was assessed after transfection with SD1211-SiSmad3-2 siRNA vector by Western blot analysis. Smad3 protein was detected as a band corresponding to 54 kDa. Expression was strong and

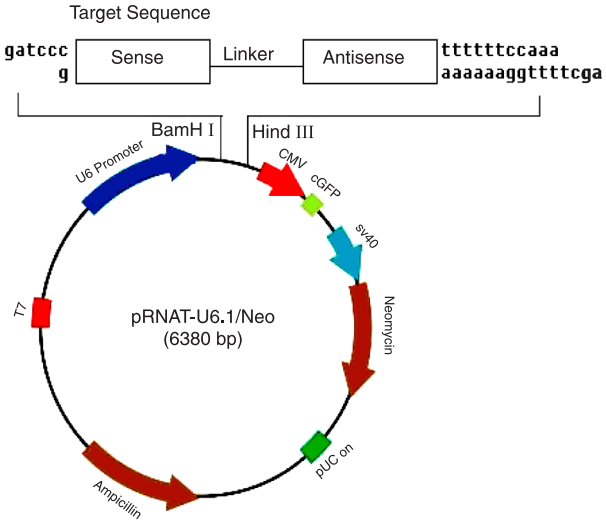

Figure 1. The siRNA expression vector pRNAT-U6.1/Neo used in the present study.

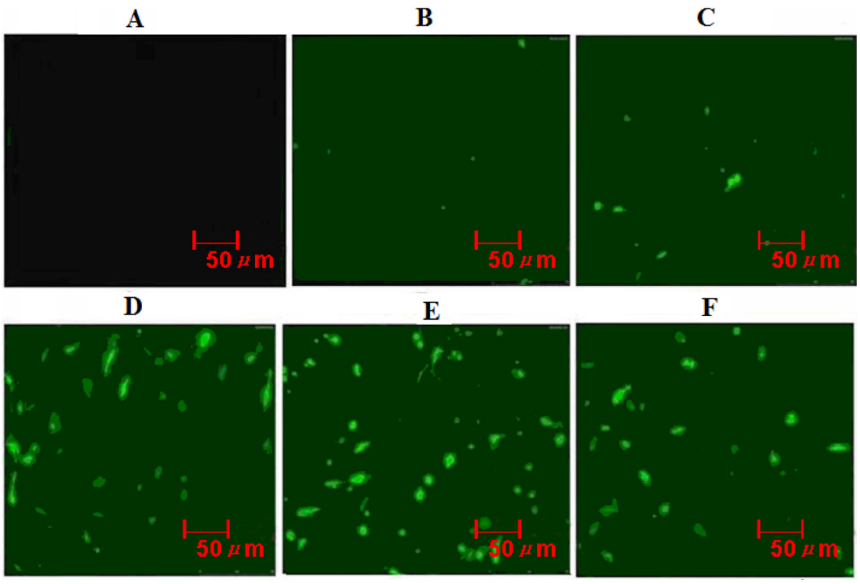

Figure 2. Fluorescence profile of hepatic stellate cells (HSCs) transfected with the Smad3 siRNA expression vector labeled with green fluorescent protein (GFP). *A*, Normal control HSCs; *B-F*, HSCs transfected with siRNA expression plasmids at 0.4, 0.6, 0.8, 1.0, 1.2 µg plasmids/10^6 cells, respectively. The expression of GFP in E (1.0 µg plasmids/10^6 cells) is powerful, which is a more suitable concentration.

clearly detected in lysates of normal HSCs, whereas in the cells transfected with the siRNA vector, the Smad3 protein was hardly expressed (Figure 4B). This result is consistent with the RT-PCR results. The siRNA expression vector clearly decreased the expression of Smad3 protein.

Changes in the mRNA expression of Smad2, 3, 4, and Col1α1, Col3α1, Col4α1

We monitored the mRNA expression levels of Smad2, 3, 4, and Col1α1, Col3α1, Col4α1 after transfection of HSCs with the SD1211-SiSmad3-2 siRNA vector. RT-PCR revealed that Smad3 expression was reduced in HSCs transfected with the Smad3 siRNA expression vector. The mRNA expression levels of Smad2, 3, 4, and Col1α1, Col3α1, Col4α1 displayed various degrees of down-regulation with little change in the Smad4 mRNA level and more obvious down-regulation of Smad2 and 3 and Col1α1, Col3α1 and Col4α1 mRNA expression (Figure 5).

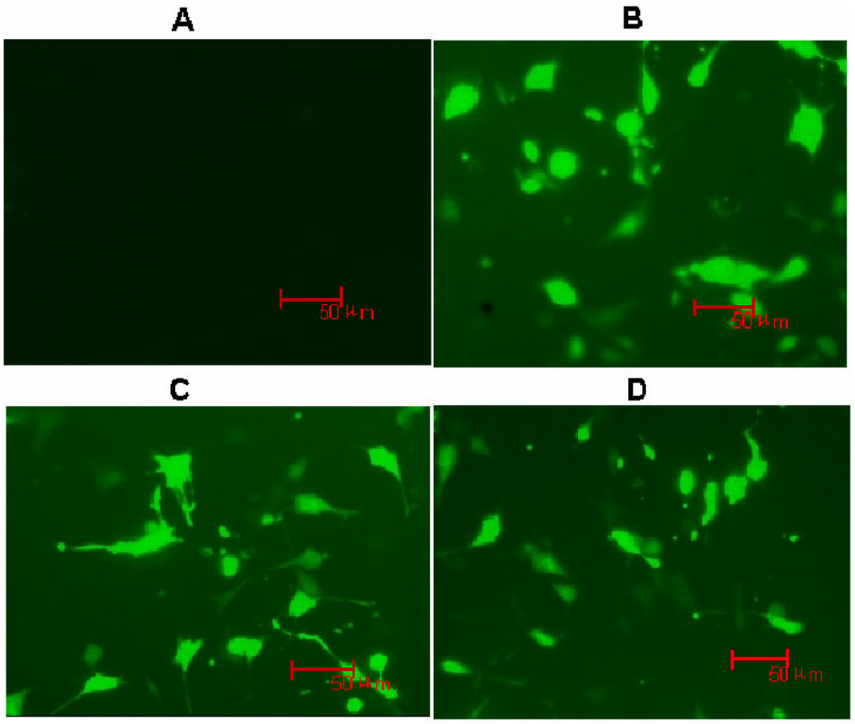

Figure 3. Fluorescence profiles of hepatic stellate cells (HSCs) transfected with three different siRNA vectors labeled with green fluorescent protein (GFP). *A*, Normal HSCs; *B-D*, HSCs transfected with three different Smad3 siRNA expression vectors at 1.0 µg plasmids/10^6 cells. The expression of GFP in *Panel C* (SD1211-SiSmad3-2) is powerful and is the best Smad3 siRNA expression vector in this study.

Effect of SD1211-SiSmad3-2 siRNA on the pathology of rat hepatic fibrosis induced by CCl_4

The results of hematoxylin and eosin staining and van Gieson collagenous fiber staining of tissue harvested at the end of the 8th week are shown in Figure 6. In the normal group, the structure of the hepatic leaflets was intact with an orderly arrangement of hepatocytes and no infiltration of inflammatory cells. In the untreated group, fat, hydropic degeneration and spotty necrosis of rat hepatocytes were observed at the end of the 6th and 8th weeks. Enhanced collagenous fiber deposition formed a complete fibrous septum, hepatic lobes were segmented into pseudolobules and chronic infiltration of inflammatory cells was observed in the fibrous septum at the end of the 8th week. In the treated group, hydropic degeneration, fat denaturation, infiltration of inflammatory cells, and enhanced deposition of collagenous fibers in liver tissues were subtle compared to the changes observed in the untreated group. The semi-quantitative scoring system value for the treated group was significantly different from that of the untreated group ($P < 0.05$). The serum indexes (PCIII, IVC, LN, HA) were also markedly higher than those of the treated group ($P < 0.01$; Tables 5 and 6).

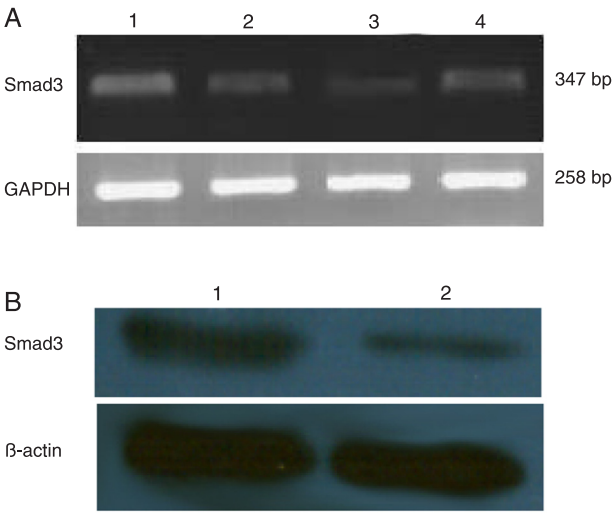

Figure 4. *A*, Smad3 mRNA expression following transfection with different Smad3 siRNA expression vectors. *Lane 1*: Normal HSC-T6; *lanes 2-4*: hepatic stellate cells (HSCs) transfected with one of three different Smad3 siRNA expression vectors. *B*, Western blot of Smad3 protein following transfection with a Smad3 siRNA expression vector. *Lane 1*: Normal HSCs; *lane 2*: HSCs transfected with the SD1211-SiSmad3-2 siRNA vector.

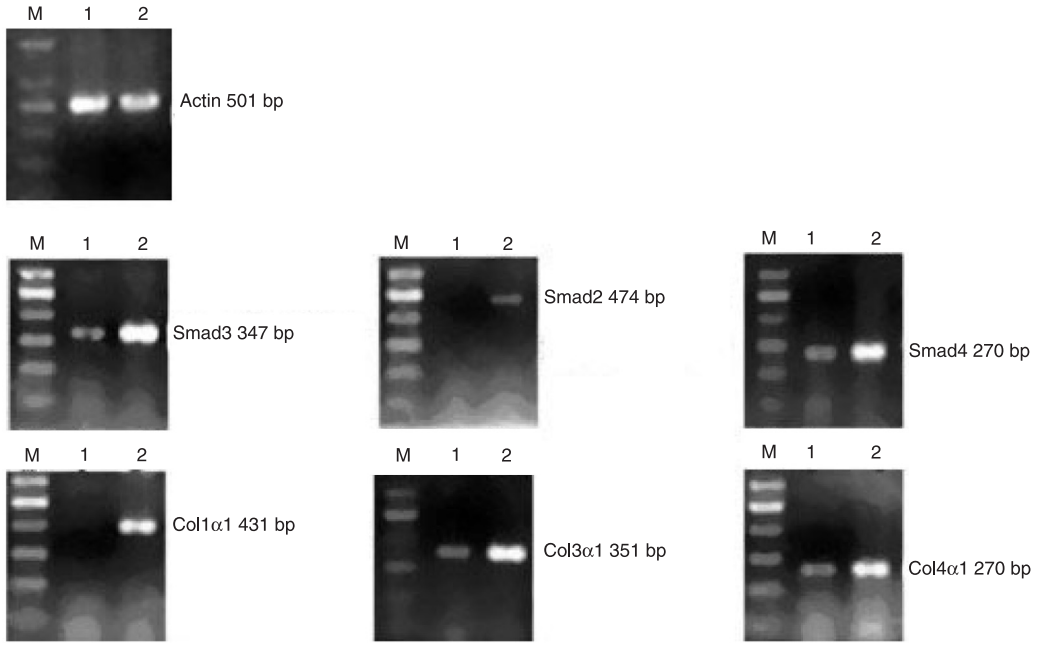

Figure 5. RT-PCR profiles of Smad2, 3, and 4, and Col1α1, Col3α1, Col4α1 mRNAs in hepatic stellate cells (HSCs) transfected with the effective Smad3 siRNA expression vector. *M*, Marker; *Lane 1*: HSCs transfected with the SD1211-SiSmad3-2 vector; *lane 2*: normal HSCs.

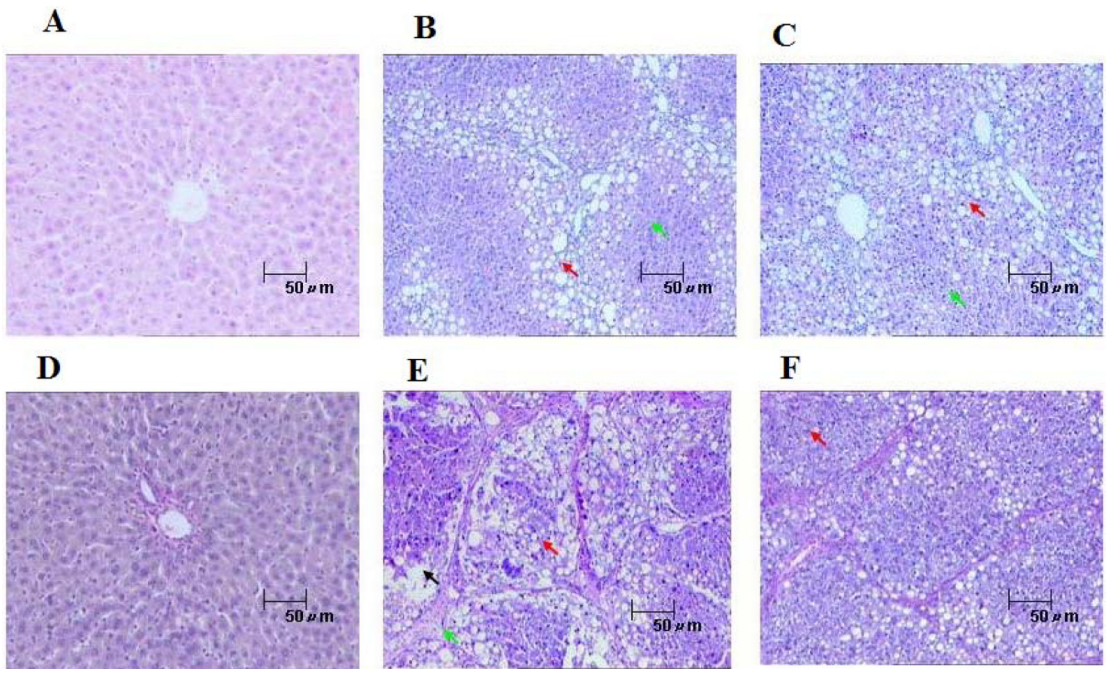

Figure 6. Hematoxylin and eosin (H&E) staining and van Gieson collagenous (VG) fiber staining. *A*, *B* and *C* were stained with H&E, in the normal control group, the untreated hepatic fibrosis group, and the treated hepatic fibrosis group, respectively; *D*, *E* and *F* were stained with VG in the three groups, respectively; *A*, *D*, a normal hepatic lobule; *B*, fatty degeneration of hepatocytes (red arrow) and abnormal hepatic lobules (green arrow), which were more visible than those in *Panel C*; *E*, pseudo-lobules (red arrow), infiltration of inflammatory cells (green arrow) and necrotic hepatocytes (black arrow); *F*, pseudo-lobules (red arrow), but less than those in *Panel E*.

Discussion

Hepatic fibrosis is a chronic pathological process characterized by ECM precipitation that is induced by many chronic pathogenic factors in the liver. On the one hand, hepatocytes are gradually damaged and ultimately die, with a reduction of their number. On the other hand, with the stimulation of numerous inflammatory factors and growth factors, interstitial cells (mainly HSCs) are activated. They gather around the affected sites with hyperplasia and secrete a large amount of ECM (e.g., collagen, fibronectin, undulin, elastin, laminin, hyaluronic acid, proteoglycan). The ECM leads to the abundant precipitation of collagen in the mesenchyme, which changes the structure of the liver.

From the viewpoint of molecular biology, the continuous activation of HSCs is a key step in hepatic fibrosis (1-6). Their ongoing activation is related to many growth factors, including TGF-β, platelet-derived growth factor (PDGF), insulin-like growth factor (IGF), fibroblast growth factor (FGF), and epidermal growth factor (EGF). Among these growth factors, TGF-β plays a particularly important role. TGF-β1 is the most important cell factor that promotes hepatic fibrosis (7-9). TGF-β1 may also promote the activation of HSCs by autocrine and paracrine pathways (18-20).

HSCs are mainly activated by the TGF-β1-Smad signaling pathway (8-11). In this pathway, TGF-β1 first combines with TGF-β1 receptors on the cell membrane. The TGF-β1 receptors are classified into three types: I, II and III, of which type I (TβRI) and type II (TβRII) play leading roles in signal transduction. TGF-β1 combines with its receptors to form a hetero-oligomeric complex of TβRII-TGF-β1-TβRI. This complex activates the downstream Smad signaling proteins (Smad2, Smad3, Smad4). The activated Smad proteins form heterodimers that enter into the nucleus and combine with specific DNA-binding proteins to regulate transcription. Thus, TGF-β1 regulates the transcription of target genes (e.g., the collagen gene). In a preliminary study, it was considered that Smad2 played an important role in HSC activation via the TGF-β1-Smad signaling pathway. Recently, it was shown that Smad3 has a strong effect on the phenotypic changes of HSCs and collagen synthesis, whereas Smad2 has an obvious effect on HSC proliferation (10-12).

The continuous activation of HSCs results in phenotypic changes such as the decreasing expression of desmin, the expression of α-smooth muscle actin (α-SMA) and intercellular adhesion molecule-1 (ICAM-1), contractility, and aggregation. In addition, HSCs will express more ECM. Therefore, the synthesis of Col1α1, Col3α1, Col4α1 is enhanced. The expression of tissue inhibitor of metalloproteinase (TIMP) is increased in order to inhibit the degradation of ECM, as well as to promote hepatic fibrosis and fibrous scar formation (21).

The animal model of hepatic fibrosis induced by carbon tetrachloride is the classical model of hepatic fibrosis. After entering into an organism, carbon tetrachloride is activated as radicals (e.g., $-CCl_3$ and $-OOCl_3$) in the liver, which can directly damage the plasma membrane, initiate the peroxidation of lipids, destroy the structure of the liver plasma membrane, cause the deformation and necrosis of liver cells, and activate HSCs. In the early

Table 5. Semi-quantitative scoring system (SSS) for hepatic fibrosis.

Group	Week	SSS score
Normal control	4, 6, 8	0
Untreated		
(m1)	4	5.30 ± 0.67
(m2)	6	10.90 ± 0.99
(m3)	8	14.50 ± 1.08
Treated		
(t1)	6	10.00 ± 0.94
(t2)	8	13.40 ± 1.07

Data are reported as means ± SD for 10 rats/group. P < 0.05 for t2 *vs* m3; P < 0.01 for m1 *vs* (m3, t2, m2, t1) and for m3 *vs* m2; P > 0.05 for t1 *vs* m2 (independent samples *t*-test).

Table 6. Hepatic fibrosis serum index for each group.

Group	Week	HA	LN	PCIII	IVC
Normal control					
	4	130.97 ± 25.14	34.74 ± 6.75	38.63 ± 7.38	51.23 ± 7.23
	6	132.62 ± 21.40	34.24 ± 6.26	39.31 ± 6.81	52.22 ± 7.19
	8	134.17 ± 23.68	36.93 ± 6.36	41.45 ± 6.53	52.73 ± 6.53
Untreated					
(m1)	4	251.57 ± 21.41	56.97 ± 7.32	73.86 ± 8.31	80.39 ± 7.29
(m2)	6	359.84 ± 61.30	96.93 ± 12.78	99.47 ± 12.00	130.07 ± 6.45
(m3)	8	518.16 ± 40.71	195.38 ± 32.50	188.97 ± 18.69	210.27 ± 18.40
Treated					
(t1)	6	335.22 ± 38.28	80.56 ± 11.49	87.30 ± 7.17	129.15 ± 11.24
(t2)	8	443.18 ± 43.40	167.06 ± 19.81	151.06 ± 11.17	149.70 ± 10.43

Data are reported as means ± SD in μg/L for 10 rats/group. HA = hyaluronic acid; LN = laminin; PCIII = type III procollagen; IVC = type IV collagen. P < 0.01 for t2 *vs* m3 for the indexes of HA, PCIII, IVC; P < 0.05 for the index of LN. P < 0.05 for t1 *vs* m2 for PCIII; P < 0.01 for LN (independent samples *t*-test).

stage, carbon tetrachloride causes acute inflammation in the liver, edema, tissue degeneration, fat degeneration, the necrosis of cell parts, and limited ECM precipitation. With continuous damage to the liver, fat degeneration gradually worsens, HSCs are persistently activated, and ECM precipitation increases. Thereafter, the aggravated fibrosis of peripheral tissue occurs and sclerosed nodes form after 8 weeks. The main feature of hepatic fibrosis is the aggregation of liver cells surrounded by fibrous tissue (22-24).

Genetic techniques, such as the use of siRNA, microRNA, antisense oligo-deoxynucleotides, and ribozymes, have been used to modulate the expression or function of TGF-β. Among these technologies, siRNA is a promising strategy for gene therapy. This technique permits the sequence-specific inhibition of gene expression (25). Sequence-specific dsRNAs can induce post-transcriptional gene silencing. After entering the cell, the dsRNA is cut into many fragments of small interfering RNAs (siRNAs). Sequence-specific siRNAs have been successfully transfected into mammalian cells to reduce the expression of specific mRNAs. Compared to gene knock-out technology, siRNA efficiently inhibits the expression of a target gene with a simple technique that is more cost effective and requires less time. This technique has become a powerful tool in the study of gene function. In this respect, it has attracted many investigators in the search of new treatments for tumors, viral infections and auto-immune diseases (26-31).

In our study, we successfully constructed an effective siRNA expression vector for Smad3. The Smad3 siRNA expression vector was transfected into rat HSCs using positive liposomes. Smad3 expression was down-regulated and signal transduction through the TGF-β1-Smad pathway was reduced. We found that downstream fibrosis index genes (e.g., Col1α1, Col3α1, Col4α1) were down-regulated more markedly after the inhibition of Smad3 expression. This result is consistent with the findings of similar experiments concerning the effects of TGFβ-Smad3 on hepatic fibrosis (32-34). Therefore, our findings support the feasibility of using siRNA to treat hepatic fibrosis. In our experiment, positive liposomes were used to transfer the siRNA expression plasmids to cells.

This approach led to a specific reduction of Smad3 gene expression *in vitro*. The Smad3 expression plasmids were transfected into a rat hepatic fibrosis model induced by carbon tetrachloride. In this model, we found that the specific knockdown of Smad3 expression had an anti-fibrotic effect, as reflected by changes in the histology of liver sections and the serum fibrosis index. However, this gene therapy is still in the experimental stage. The safe and effective transfection of the vector into target tissue cells remains a challenge. Our study provides a theoretical basis for gene therapy for hepatic fibrosis in chronic hepatopathy.

Acknowledgments

Research supported by the Suzhou Social Development Program (#SS0703).

References

1. Rosenbloom J, Castro SV, Jimenez SA. Narrative review: fibrotic diseases: cellular and molecular mechanisms and novel therapies. *Ann Intern Med* 2010; 152: 159-166.
2. Gressner AM, Weiskirchen R. Modern pathogenetic concepts of liver fibrosis suggest stellate cells and TGF-beta as major players and therapeutic targets. *J Cell Mol Med* 2006; 10: 76-99.
3. Bataller R, Brenner DA. Liver fibrosis. *J Clin Invest* 2005; 115: 209-218.
4. Wells RG. The role of matrix stiffness in hepatic stellate cell activation and liver fibrosis. *J Clin Gastroenterol* 2005; 39: S158-S161.
5. Bataller R, Brenner DA. Hepatic stellate cells as a target for the treatment of liver fibrosis. *Semin Liver Dis* 2001; 21: 437-451.
6. Pinzani M, Marra F. Cytokine receptors and signaling in hepatic stellate cells. *Semin Liver Dis* 2001; 21: 397-416.
7. Cutroneo KR. TGF-beta-induced fibrosis and SMAD signaling: oligo decoys as natural therapeutics for inhibition of tissue fibrosis and scarring. *Wound Repair Regen* 2007; 15 (Suppl 1): S54-S60.
8. Matsuzaki K. Modulation of TGF-beta signaling during progression of chronic liver diseases. *Front Biosci* 2009; 14: 2923-2934.
9. Gressner AM, Weiskirchen R, Breitkopf K, Dooley S. Roles of TGF-beta in hepatic fibrosis. *Front Biosci* 2002; 7: d793-d807.
10. Flanders KC. Smad3 as a mediator of the fibrotic response. *Int J Exp Pathol* 2004; 85: 47-64.
11. Uemura M, Swenson ES, Gaca MD, Giordano FJ, Reiss M, Wells RG. Smad2 and Smad3 play different roles in rat hepatic stellate cell function and alpha-smooth muscle actin organization. *Mol Biol Cell* 2005; 16: 4214-4224.
12. Callahan JF, Burgess JL, Fornwald JA, Gaster LM, Harling JD, Harrington FP, et al. Identification of novel inhibitors of the transforming growth factor beta1 (TGF-beta1) type 1 receptor (ALK5). *J Med Chem* 2002; 45: 999-1001.
13. Landen CN Jr, Chavez-Reyes A, Bucana C, Schmandt R, Deavers MT, Lopez-Berestein G, et al. Therapeutic EphA2 gene targeting *in vivo* using neutral liposomal small interfering RNA delivery. *Cancer Res* 2005; 65: 6910-6918.
14. Bartlett DW, Davis ME. Insights into the kinetics of siRNA-mediated gene silencing from live-cell and live-animal bioluminescent imaging. *Nucleic Acids Res* 2006; 34: 322-333.
15. Chevallier M, Guerret S, Chossegros P, Gerard F, Grimaud JA. A histological semiquantitative scoring system for evaluation of hepatic fibrosis in needle liver biopsy specimens: comparison with morphometric studies. *Hepatology* 1994; 20: 349-355.
16. Wang TL, Liu X, Zhou YP, He JW, Zhang J, Li LZ, et al. A

semiquantitative scoring system for assessment of hepatic inflammation and fibrosis in chronic viral hepatitis. *Chin J Hepatol* 1998; 6: 195-197.
17. Qiu JF, Zhang ZQ, Chen W, Wu ZY. Cystamine ameliorates liver fibrosis induced by carbon tetrachloride via inhibition of tissue transglutaminase. *World J Gastroenterol* 2001; 7: 42-48.
18. Parsons CJ, Takashima M, Rippe RA. Molecular mechanisms of hepatic fibrogenesis. *J Gastroenterol Hepatol* 2007; 22 (Suppl 1): S79-S84.
19. Breitkopf K, Lahme B, Tag CG, Gressner AM. Expression and matrix deposition of latent transforming growth factor beta binding proteins in normal and fibrotic rat liver and transdifferentiating hepatic stellate cells in culture. *Hepatology* 2001; 33: 387-396.
20. Breitkopf K, Godoy P, Ciuclan L, Singer MV, Dooley S. TGF-beta/Smad signaling in the injured liver. *Z Gastroenterol* 2006; 44: 57-66.
21. Safadi R, Friedman SL. Hepatic fibrosis - role of hepatic stellate cell activation. *MedGenMed* 2002; 4: 27.
22. Ogeturk M, Kus I, Pekmez H, Yekeler H, Sahin S, Sarsilmaz M. Inhibition of carbon tetrachloride-mediated apoptosis and oxidative stress by melatonin in experimental liver fibrosis. *Toxicol Ind Health* 2008; 24: 201-208.
23. Lee GP, Jeong WI, Jeong DH, Do SH, Kim TH, Jeong KS. Diagnostic evaluation of carbon tetrachloride-induced rat hepatic cirrhosis model. *Anticancer Res* 2005; 25: 1029-1038.
24. Fu Y, Zheng S, Lin J, Ryerse J, Chen A. Curcumin protects the rat liver from CCl4-caused injury and fibrogenesis by attenuating oxidative stress and suppressing inflammation. *Mol Pharmacol* 2008; 73: 399-409.
25. Meister G, Tuschl T. Mechanisms of gene silencing by double-stranded RNA. *Nature* 2004; 431: 343-349.
26. Medema RH. Optimizing RNA interference for application in mammalian cells. *Biochem J* 2004; 380: 593-603.
27. Sioud M. On the delivery of small interfering RNAs into mammalian cells. *Expert Opin Drug Deliv* 2005; 2: 639-651.
28. Ryther RC, Flynt AS, Phillips JA III, Patton JG. siRNA therapeutics: big potential from small RNAs. *Gene Ther* 2005; 12: 5-11.
29. Hannon GJ, Rossi JJ. Unlocking the potential of the human genome with RNA interference. *Nature* 2004; 431: 371-378.
30. Dorsett Y, Tuschl T. siRNAs: applications in functional genomics and potential as therapeutics. *Nat Rev Drug Discov* 2004; 3: 318-329.
31. Caplen NJ, Mousses S. Short interfering RNA (siRNA)-mediated RNA interference (RNAi) in human cells. *Ann N Y Acad Sci* 2003; 1002: 56-62.
32. Henderson NC, Mackinnon AC, Farnworth SL, Poirier F, Russo FP, Iredale JP, et al. Galectin-3 regulates myofibroblast activation and hepatic fibrosis. *Proc Natl Acad Sci U S A* 2006; 103: 5060-5065.
33. Inagaki Y, Higashi K, Kushida M, Hong YY, Nakao S, Higashiyama R, et al. Hepatocyte growth factor suppresses profibrogenic signal transduction via nuclear export of Smad3 with galectin-7. *Gastroenterology* 2008; 134: 1180-1190.
34. Xu W, Wang LW, Shi JZ, Gong ZJ. Effects of RNA interference targeting transforming growth factor-beta 1 on immune hepatic fibrosis induced by Concanavalin A in mice. *Hepatobiliary Pancreat Dis Int* 2009; 8: 300-308.